Localized modes in finite and phase-inhomogeneous Josephson tunnel junctions

A. K. Setty and Gabriele F. Giuliani
Department of Physics, Purdue University, West Lafayette, Indiana 47907-1396
(Received 16 February 1999)

We have investigated the spectrum of localized modes in both finite and phase inhomogeneous long one-dimensional Josephson junctions in the presence of an external magnetic field. For finite junctions these excitations correspond to evanescent waves localized near the edges. Both the frequency and the characteristic decay lengths depend on the magnetic field. In particular, a different behavior is expected for the Meissner state and the mixed state in which wholesale penetration of Josephson vortices occurs. The related problem of the spectrum of modes localized near phase inhomogeneities occurring well inside a long junction has been also tackled. This problem is relevant to the case in which Abrikosov vortices penetrate the electrodes and become pinned near the junction plane.

I. INTRODUCTION

There have been numerous studies[1–4] of the electrodynamics of Josephson junctions with various geometries, such as those with infinite, semi-infinite, and finite widths, with a view to studying the collective modes in these systems. This problem is of great importance vis a vis its implications on the behavior of the current voltage characteristic. Recently, considerable interest has developed in phase inhomogeneous junctions.[5–15] Hence we discuss here the case of a long Josephson tunnel junction with phase inhomogeneity, and establish the existence and the physical properties of small amplitude localized modes analogous to the surface states[16] that occur in the semi-infinite junctions. In order to describe our results we found it necessary to reexamine and carefully discuss the physics for the case of infinite and semi-infinite junctions. The static phase solutions, the spectrum of small oscillations and the associated decay lengths of the wave functions are presented in both the Meissner and the mixed states.

We consider a long Josephson junction consisting of two superconducting electrodes of semi-infinite cross section with a thin dielectric interface of thickness d lying in the xy plane. The geometry of the situation is depicted in Fig. 1. The fundamental equation for the phase dynamics is[17,18]

$$\Delta\varphi(x,y,t)-\frac{1}{c_0^2}\frac{\partial^2\varphi(x,y,t)}{\partial^2 t^2}=\frac{\sin\varphi(x,y,t)}{\lambda_J^2}, \qquad (1)$$

where $c_0=c\sqrt{d/\epsilon l}$, is the velocity of the Swihart waves[19] and as usual $\lambda_J=\sqrt{\hbar c^2/8\pi e j_c l}$ is the Josephson penetration depth. Here l, which is the thickness of the region containing the magnetic fields, is given by $l=2\lambda_L+d$, where λ_L is the London penetration depth.

To study the dynamics of small phase oscillations it is convenient to express the Josephson phase in terms of the finite static component $\varphi_0(x)$ plus a small perturbation $\tilde{\varphi}_1(x,y,t)$. The substitution $\varphi=\varphi_0(x)+\tilde{\varphi}_1(x,y,t)$, leads to the following equations for the static phase and the amplitude of the small oscillations:

$$\Delta\varphi_0(x)=\frac{\sin\varphi_0(x)}{\lambda_J^2}, \qquad (2)$$

$$\left[\Delta-\frac{1}{c_0^2}\frac{\partial^2}{\partial t^2}\right]\tilde{\varphi}_1(x,y,t)=\frac{\cos\varphi_0(x)}{\lambda_J^2}\tilde{\varphi}_1(x,y,t). \qquad (3)$$

These equations alongside the appropriate boundary conditions required by the presence of an externally applied magnetic field, determine the collective modes of the junction. In Sec. II we review the case of an infinite junction and set the stage for the description of the modes of semi-infinite systems. The latter are explicitly discussed in Sec. III where

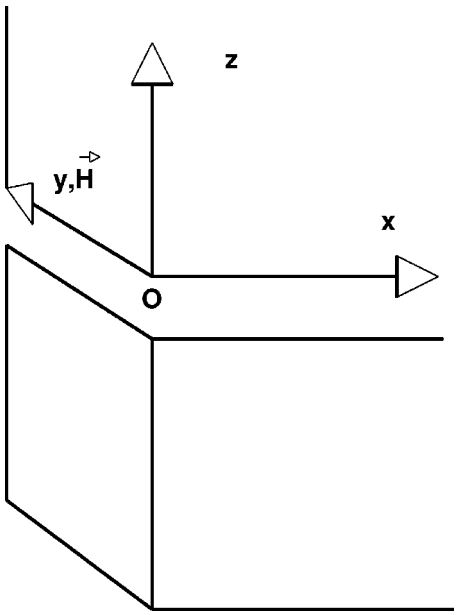

FIG. 1. Schematic of a semi-infinite Josephson junction in which the interface with vacuum is the y,z plane at $x=0$. The system is assumed to extend to infinity along the positive x axis. A magnetic field is applied along the y direction and even in the Meissner state will modify the Josephson phase near the interface. In the mixed state a periodic structure of Josephson vortices will be present for $x\geqslant 0$.

the approach of Ref. 4 is extended to extract and characterize the behavior of the decay lengths with the magnetic field. In Sec. IV, we consider the problem of a phase impurity in a long Josephson junction. The final section presents a comparison of the different geometries and a physical discussion of the results.

II. COLLECTIVE MODES IN INFINITE JOSEPHSON JUNCTIONS

The long wavelength spectrum for the small phase oscillations in a long Josephson tunnel junction was obtained by Kulik.[1,18] Kulik's results were generalized for all wavelengths by Lebwohl and Stephen[2] and subsequently by Fetter and Stephen.[3]

The Meissner state solution of Eq. (2) is simply $\varphi_0(x)=0$, while the corresponding solution for the mixed state is given by

$$\sin\left(\frac{\varphi_0(x)-\pi}{2}\right)=sn\left(\frac{x}{\gamma},\gamma\right), \tag{4}$$

where sn is a Jacobian elliptic function with the quantity γ as its modulus.[20,21] In view of the periodic properties of the function sn, this solution describes a line of Josephson vortices with lattice spacing given by $a=2\gamma K(\gamma)\lambda_J$ along the x axis. Here $K(\gamma)$ is the complete elliptic integral of first kind.[22] Here γ introduces a suitable parametrization for the induction and is related to the externally applied field H via the relation $H/H_1=4E(\gamma)/\pi\gamma$, where $H_1=\phi_0/4\pi\lambda_J\lambda_L$, with ϕ_0 the quantum of flux, is a characteristic field scale of the junction. In particular $\gamma\to 0$ corresponds to the infinite field limit ($a\to 0$), while the limit $\gamma\to 1$ corresponds to the bulk lower critical field value of $H_{c1}=4H_1/\pi=2\phi_0/\pi^2\lambda_l\lambda_J$, as the vortex separation a diverges.

The next step is to make the following substitution into the equation for the small oscillations:

$$\tilde{\varphi}_1(x,y,t)=\varphi_1(x)e^{iky-i\omega t}, \tag{5}$$

which leads to

$$\left[\frac{d^2}{dx^2}+\frac{\omega^2}{c_0^2}-k^2\right]\varphi_1(x)=\frac{\cos\varphi_0(x)}{\lambda_J^2}\varphi_1(x). \tag{6}$$

At this point it is convenient to recast Eqs. (2) and (6) in dimensionless form. With $x/\lambda_J\to x$, and $k\lambda_J\to k$, we obtain

$$\Delta\varphi_0(x)=\sin\varphi_0(x) \tag{7}$$

and

$$\left[\frac{d^2}{dx^2}+\frac{\omega^2}{\omega_J^2}-k^2\right]\varphi_1(x)=\cos\varphi_0(x)\varphi_1(x), \tag{8}$$

where we have introduced the Josephson plasma frequency $\omega_J=c_0/\lambda_J$.

It is clear that in the case of no field penetration (i.e., the Meissner state) $\varphi_0(x)$ vanishes everywhere and the spectrum of the collective modes is simply given by

$$\omega^2=\omega_J^2(1+k^2+q^2). \tag{9}$$

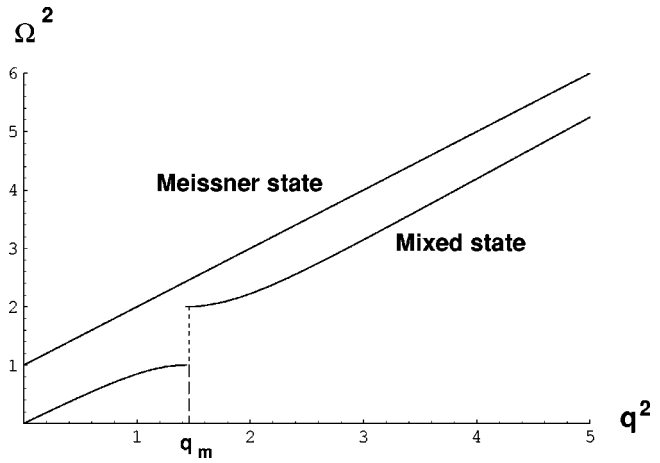

FIG. 2. Collective spectrum for an infinite junction. Here the reduced frequency $\Omega^2=\omega^2/\omega_J^2-k^2$ is plotted vs the square of the reduced wave vector q along the x axis. The continuous upper curve corresponds to the Meissner state. The gapped lower curve corresponds to the mixed state for an external magnetic field corresponding to $\gamma=2^{-1/2}$, where the parameter γ is defined in the text.

This spectrum is depicted in Fig. 2 (upper curve) where the reduced frequency $\Omega^2=\omega^2/\omega_J^2-k^2$ is plotted against q^2.

As the field penetrates the junction (i.e., the mixed state) the situation is far more complex as, for the present geometry, the field takes the form of a periodic one dimensional lattice of Josephson vortices. While Kulik[1] limited his analysis to a small wave vector expansion of Eq. (8), Lebwohl and Stephen[2] established for this case the exact solution for the phase amplitude in the form

$$\varphi_1(x)=u_q(x)e^{iqx}, \tag{10}$$

where the $u_q(x)$ are here suitable Bloch functions, and full advantage is taken of the double periodicity of the elliptic functions.[20,22] Here q is the dimensionless wave vector rescaled by the Josephson penetration depth.

In this case the spectrum is comprised of two bands separated by the only gap located at $q_m=\pm\pi/a=\pm\pi/2\gamma K(\gamma)$. The lower band can be described in terms of Josephson vortex oscillations, while the upper one can be seen to correspond to plasma modes.

The lower branch (the vortex oscillations) is described by a Bloch function given by

$$u_q(x)=\frac{\vartheta_3\left[\frac{\pi x}{2\gamma K(\gamma)}+\frac{i\pi\chi_q}{2K(\gamma)}\middle|\tau\right]}{\vartheta_4\left[\frac{\pi x}{2\gamma K(\gamma)}\middle|\tau\right]}, \tag{11}$$

where the ϑ_i's are elliptic theta functions and $\tau=iK'/K(\gamma)$, with $K'=K(\gamma')$ and $\gamma'=\sqrt{1-\gamma^2}$. The Bloch function depends on q parametrically via the variable χ_q, which is determined via the relation

$$q=\frac{1}{\gamma}\left[E(\chi_q,\gamma')-\chi_q\left(1-\frac{E(\gamma)}{K(\gamma)}\right)\right], \tag{12}$$

where $E(\chi_q,\gamma')$ is the incomplete Jacobi elliptic integral of the second kind.[20,22] As χ_q varies between 0 and K', q varies between 0 and q_m.

The dispersion relation corresponding to this lower branch is found to be given by

$$\omega^2=c_0^2\left[k^2+\frac{\gamma'^2}{\gamma^2}sn^2(\chi_q,\gamma')\right]. \tag{13}$$

In the same way, the plasma oscillations have a Bloch function given by

$$u_q(x)=\frac{\vartheta_4\left[\frac{\pi x}{2\gamma K(\gamma)}-\frac{i\pi}{2K(\gamma)}(\chi_q-K')\middle|\tau\right]}{\vartheta_4\left[\frac{\pi x}{2\gamma K(\gamma)}\middle|\tau\right]}, \tag{14}$$

where now, for $q\geqslant q_m$

$$q-q_m=\frac{1}{\gamma}\left[-E(\chi_q,\gamma')+\chi_q\left(1-\frac{E(\gamma)}{K(\gamma)}\right)+\frac{dn(\chi_q,\gamma')sn(\chi_q,\gamma')}{cn(\chi_q,\gamma')}\right], \tag{15}$$

where the remaining Jacobian elliptic functions now appear.[20]

The corresponding dispersion is given by

$$\omega^2=c_0^2\left[k^2+\frac{1}{\gamma^2}\frac{dn^2(\chi_q,\gamma')}{cn^2(\chi_q,\gamma')}\right]. \tag{16}$$

The complete spectrum in the mixed state is shown in Fig. 2 for $\gamma=1/\sqrt{2}$.

An expansion in q near q_m leads to an expression for the gap:

$$[\omega^2_{\text{vortex}}-\omega^2_{\text{plasma}}]_{q=q_m}=\omega_J^2, \tag{17}$$

which is seen to be independent of the magnetic field and to coincide with that of the Meissner state spectrum (i.e., the Josephson plasma frequency). It is significant for what follows that as γ tends to unity, the position of the gap shifts in the Ω^2 vs q^2 plane and evolves into the Meissner gap at $\gamma=1$, the vortex oscillations branch disappearing.

III. SURFACE LOCALIZED MODES IN JOSEPHSON JUNCTIONS

We consider next a semi-infinite Josephson junction with a surface in the y,z plane at $x=0$. In this instance we solve Eqs. (7) and (8), subject to the boundary conditions

$$\left.\frac{d\varphi_0}{dx}\right|_{x=0,L}=H_0 \tag{18}$$

and

$$\left.\frac{d\varphi_1}{dx}\right|_{x=0,L}=0, \tag{19}$$

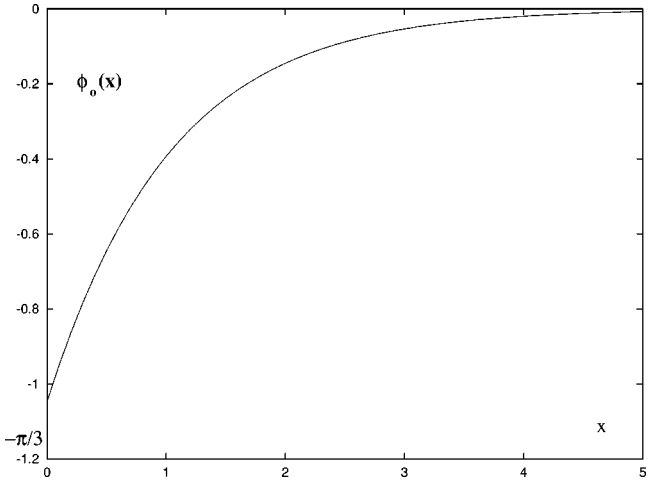

FIG. 3. The spatial variation of the static phase in the Meissner regime for a surface localized mode ($h=0.5$).

where $H_0=H/H_1$, and H_1 was defined below Eq. (4). Furthermore, since we seek evanescent wave solutions, we also have $\varphi_1(\infty)=0$.

The Meissner state solution of Eq. (7) which corresponds to the minimum energy is given by (see Fig. 3)

$$\varphi_0(x)=-2\arcsin\left\{\frac{1}{\cosh[x+C(h)]}\right\}, \tag{20}$$

where $C(h)=\cosh^{-1}1/h$, and we have introduced the field scale $h=H/H_s=H_0/2$. Here H_s is the superheating field, representing the maximum external field value for which the above Meissner state solution can be still made to satisfy Eq. (18) thereby establishing a metastable situation. H_s is readily found to be given here by $2H_1$ and is therefore larger than the bulk lower critical field $H_{c1}=4H_1/\pi\simeq 1.27H_1$.

In the mixed state the static value of the phase is given by a simple generalization of Eq. (4), i.e.,

$$\sin\left(\frac{\varphi_0(x)-\varphi_0(0)}{2}\right)=sn\frac{x}{\gamma}, \tag{21}$$

where $\varphi_0(0)$ is determined from the condition (18). As it turns out, the solution with the lowest energy corresponds in this case to the value

$$\varphi_0(0)=-2\arccos\sqrt{\frac{1}{\gamma^2}-\frac{H_0^2}{4}}. \tag{22}$$

It is useful to rewrite Eq. (21) as follows:

$$\cos\frac{\varphi_0(x)}{2}=sn\left(\frac{x-A(\gamma)}{\gamma}\right), \tag{23}$$

where we have defined

$$A(\gamma)=\gamma K\left[\frac{\pi}{2}-\frac{\varphi_0(0)}{2},\gamma\right],$$

representing the virtual location of the maximum of the magnetic field closest to the junction edge. In this expression $K(\varphi,\gamma)$ is the incomplete elliptic integral of the first kind.

Equation (7) in the form of a Schrödinger-like equation

$$\frac{\partial^2\varphi_1(x)}{\partial x^2}+2\left[\varepsilon+\gamma^2 cn^2\left(\frac{x-A(\gamma)}{\gamma},\gamma\right)\right]\varphi_1(x)=0. \quad (24)$$

Here $\varepsilon=\gamma^2/2(\omega^2/\omega_J^2-k^2-1)$. The last equation can be rewritten as a Lamé equation[20]

$$\frac{\partial^2\varphi_1(x)}{\partial x^2}=\left[2\gamma^2 sn^2\left(\frac{x-A(\gamma)}{\gamma}\right)+\gamma^2\left(k^2-\frac{\omega^2}{\omega_J^2}-1\right)\right]\varphi_1(x), \quad (25)$$

with solution

$$\varphi_1(x)=\frac{H\left[\frac{x-A}{\gamma}-\beta\right]}{\Theta\left[\frac{x-A}{\gamma}\right]}e^{-(x-A)/\gamma\lambda}, \quad (26)$$

provided the conditions

$$\frac{cn^2\beta dn^2\beta}{sn^2\beta}-\frac{1}{sn^2\beta}=\gamma^2\left(k^2-\frac{\omega^2}{\omega_J^2}-1\right), \quad (27)$$

and

$$\lambda=-Z^{-1}(\beta,\gamma) \quad (28)$$

where $Z(\beta,\gamma)=E(\beta,\gamma)-\beta[E(\gamma)/K(\gamma)]$, is the Jacobi Zeta function, are satisfied.

In Eq. (26) we have introduced the decay length λ in units of λ_J. This important length scale characterizes the spatial dependence of the phase evanescent waves.

The corresponding expression for the frequency is obtained from Eq. (27) and is given by

$$\Omega^2=\frac{dn^2\beta}{\gamma^2}. \quad (29)$$

Utilizing the boundary condition of Eq. (19) yields an equation for the parameter β. After lengthy manipulations involving Eq. (28) we arrive at the expression

$$\frac{cn\left(\beta+\frac{A}{\gamma}\right)dn\left(\beta+\frac{A}{\gamma}\right)}{sn\left(\beta+\frac{A}{\gamma}\right)}-\gamma^2 sn\beta sn\frac{A}{\gamma}sn\left(\beta+\frac{A}{\gamma}\right)=0. \quad (30)$$

By making use of the transformation properties of the Jacobian elliptic functions, it is possible to rewrite Eq. (30) as a cubic equation[23]

$$[(1-u^2)(1-\gamma^2u^2)(1-t^2)(1-\gamma^2t^2)]=u^2t^2[1+\gamma^2(1-u^2-t^2)]^2, \quad (31)$$

where $u^2=1/\gamma^2-h^2$, and $t=sn\beta=\sqrt{1/\gamma^2-\Omega^2}$. The roots of this equation are as follows:

$$\Omega_0^2=\frac{1}{\gamma^2}\frac{h^2-h_{\min}^2}{h^2-h_{\max}^2}, \quad (32)$$

where $h_{\min}=\sqrt{1-\gamma^2}/\gamma$ and $h_{\max}=1/\gamma$, and

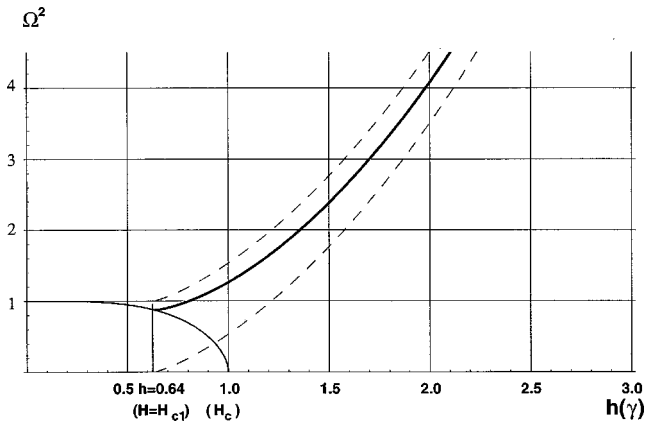

FIG. 4. The reduced frequency Ω^2 as a function of the magnetic field for a semi-infinite junction in the mixed (heavy line) and Meissner (thin line) states. The dashed curves delimit the gap in the spectrum of the infinite system. The bulk critical field H_{c1} and the superheating field H_s are indicated. The notation is the same as in Fig. 2.

$$\Omega_{\pm}^2=\frac{1}{2\gamma^2}[2-\gamma^2(1+h^2)\pm\gamma\sqrt{\gamma^2(1-h^2)^2+4h^2(1-\gamma^2h^2)}]. \quad (33)$$

Clearly Ω_0^2 and Ω_-^2 correspond to unstable solutions, so that we are left with Ω_+^2 as the only acceptable result.

We note at this point that the frequency corresponding to the Meissner state can simply be determined from the general expression for Ω_+^2 [Eq. (33)] in the limit of $\gamma\to1$. Accordingly

$$\Omega_{\text{Meissner}}^2=\frac{1}{2}[1-h^2+\sqrt{(1-h^2)^2+4h^2(1-h^2)}]. \quad (34)$$

The frequencies in the Meissner and mixed states have been plotted in Fig. 4 as a function of the applied magnetic field. Here the expression $h(\gamma)=2E(\gamma)/\pi\gamma$ for the infinite system is used.

In order to set the stage for the discussion contained in the next section it is important to study here the behavior of the decay length. From Eq. (28) we can write

$$\frac{1}{\lambda}=\int_0^{\arcsin(\sqrt{1-dn^2\beta}/\gamma)}\sqrt{1-\gamma^2\sin^2\phi}\,d\phi-\frac{E(\gamma)}{K(\gamma)}\int_0^{\arcsin(\sqrt{1-dn^2\beta}/\gamma)}\frac{d\phi}{\sqrt{1-\gamma^2\sin^2\phi}}, \quad (35)$$

where, in turn, the appropriate expression for $dn^2(\beta,\gamma)$ in the Meissner or the mixed state, is obtained respectively from Eq. (34) and (33) (taken with the plus sign) via Eq. (29).

The decay lengths in the mixed and Meissner states are plotted against the reduced frequency in Figs. 5 and 6. The corresponding decay lengths are always real and seen to lie within the gap of the spectrum for the infinite system. Hence in the circumstances that we have here discussed, the disper-

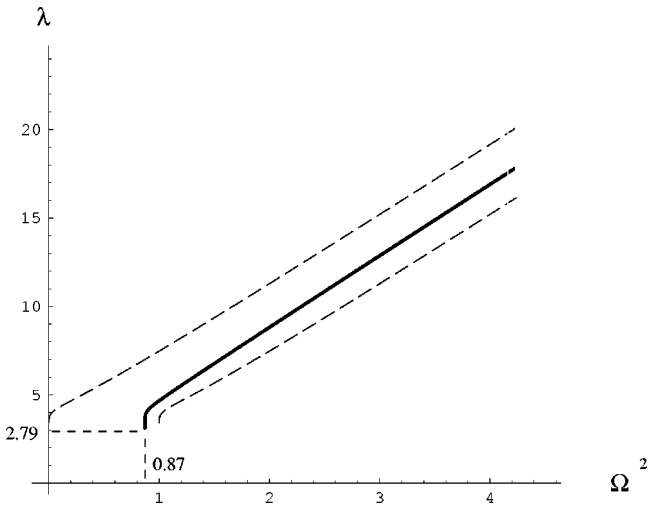

FIG. 5. Localized modes decay length vs the reduced frequency Ω^2 (heavy line) for the semi-infinite system in the mixed state. The localized modes are seen to always lie in the gap of the infinite system spectrum. The indicated point corresponds to $H=H_{c1}$. The associated decay length and frequency are the same as for the corresponding point on the plot of λ_J vs Ω^2 for the Meissner state. The dashed curves delimit the gap in the spectrum of the infinite system. The notation is the same as in Fig. 2.

sion of phase surface waves do not enter the infinite system continuum and therefore are well defined for all magnetic fields.

IV. PHASE-IMPURITY LOCALIZED MODES IN LONG JOSEPHSON JUNCTIONS

We can picture a phase impurity in a long Josephson junction by imagining that an Abrikosov vortex parallel to the y axis is pinned in the immediate vicinity of the junction plane. This vicinal Abrikosov vortex modifies the properties of the junction. A suitable model for the description of this situation is provided by the following modified equation for the static phase

$$\frac{d^2\varphi_0(x)}{dx^2}=\sin\varphi_0(x)+\psi\delta'(x-x_0), \tag{36}$$

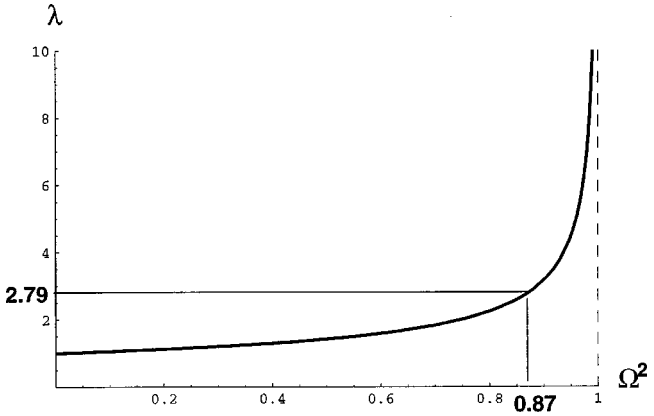

FIG. 6. Localized modes decay length vs the reduced frequency Ω^2 for a semi-infinite junction in the Meissner state. The notation is the same as in Fig. 2.

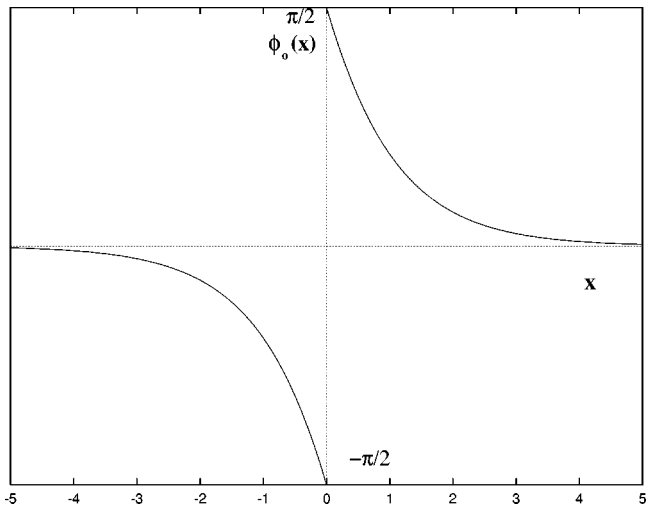

FIG. 7. The spatial variation of the static phase in the Meissner regime for a phase inhomogeneous junction ($\psi=\pi$).

where the vicinal Abrikosov vortex is located at x_0 and the coupling is taken to be proportional to the first derivative of the delta function and to have a strength ψ.[12–14]

The static phase in the Meissner state to the left and the right of the the position of the inhomogeneity is given by (see Fig. 7):

$$\varphi_0(x)=\pm 4\arctan\left(e^{\mp(x-x_0)}\tan\frac{\psi}{8}\right), \tag{37}$$

an expression that represents the localized phase distortion associated with the vicinal Abrikosov vortex.[24]

In view of the fact that the spectrum for both the Meissner and the mixed state can be obtained from the general expression appropriate to the latter, we focus next on the mixed state. In this case the general static solution is given by

$$\sin\left(\frac{\varphi_0^{\pm}(x)-\varphi_0^{\pm}(x_0^{\pm})}{2}\right)=sn\left(\frac{x-x_0}{\gamma}\right), \tag{38}$$

where $\varphi_0^{\pm}(x)$ is the static phase to the right and left of the position of the inhomogeneity. Because of the phase discontinuity introduced by the coupling with the impurity this equation becomes

$$\sin\left(\frac{\varphi_0^{\pm}(x)}{2}\pm\frac{\psi}{4}\right)=sn\left(\frac{x-x_0}{\gamma}\right). \tag{39}$$

At this point, by proceeding as in the case discussed in the previous section, we then obtain

$$\cos\frac{\varphi_0(x)}{2}=sn\left(\frac{x-x_0\pm B(\gamma)}{\gamma}\right), \tag{40}$$

where $B(\gamma)=\gamma K(\pi/2-\psi/4,\gamma)$.

The amplitude of the corresponding small oscillations are found to satisfy the equation

$$\frac{\partial^2\varphi_1(x)}{\partial x^2}=\left\{2\gamma^2 sn^2\left(x-x_0\pm\frac{B(\gamma)}{\gamma}\right)+\gamma^2\left(k^2-\frac{\omega^2}{\omega_J^2}-1\right)\right\}\varphi_1(x), \tag{41}$$

with solutions given by

$$\varphi_1^{\pm}(x)=\frac{H\left[\dfrac{(x-x_0\pm B)}{\gamma}-\beta_{\pm}\right]}{\Theta\left[\dfrac{(x-x_0\pm B)}{\gamma}\right]}e^{\mp(x-x_0\pm B)/\gamma\lambda}. \tag{42}$$

At this point, the only unknown quantity in this expression is $\beta_{\pm}$, which we now determine by imposing the requirement that magnetic field be continuous across the phase discontinuity. This condition is expressed by the relation

$$\left.\frac{d}{dx}(\varphi_0+\tilde{\varphi}_1)\right|_{x=x_0^+}=\left.\frac{d}{dx}(\varphi_0+\tilde{\varphi}_1)\right|_{x=x_0^-}. \tag{43}$$

By means of Eq. (40) we have

$$\left.\frac{d\varphi_0}{dx}\right|_{x_0^{\pm}}=-\sqrt{1-\gamma^2\cos^2\varphi_0\left(\frac{x_0^{\pm}}{2}\right)}=-\sqrt{1-\gamma^2\cos^2\frac{\psi}{4}}, \tag{44}$$

which implies continuity of $d\varphi_1/dx$ at x_0. This, in view of Eq. (42), leads to the condition

$$R(\gamma)=\frac{H[-\beta_+ +B(\gamma)/\gamma]}{H[-\beta_- -B(\gamma)/\gamma]}=\frac{F_+ +G_+ -1/\lambda}{F_- +G_- +1/\lambda}, \tag{45}$$

where

$$F_{\pm}=\left[E(-\beta_{\pm})\pm\gamma^2 sn\beta_{\pm}sn\frac{B(\gamma)}{\gamma}sn\left(-\beta_{\pm}\pm\frac{B(\gamma)}{\gamma}\right)\right] \tag{46}$$

and

$$G_{\pm}=\left[\frac{cn\left(-\beta_{\pm}\pm\dfrac{B(\gamma)}{\gamma}\right)dn\left(-\beta_{\pm}\pm\dfrac{B(\gamma)}{\gamma}\right)}{sn\left(-\beta_{\pm}\pm\dfrac{B(\gamma)}{\gamma}\right)}+\beta_{\pm}\frac{E(\gamma)}{K(\gamma)}\right]. \tag{47}$$

To ensure that φ_1 decays on both sides of the discontinuity, it is necessary to choose $\beta_-=-\beta_+$ which results in a condition on β_+ totally equivalent to Eq. (30). This leads in turn to a cubic equation identical to that of Eq. (31), where now $u^2=sn^2[B(\gamma)/\gamma]=\cos^2(\psi/4)$. By direct inspection the roots of this polynomial are in this case found to be

$$\Omega_0^2=-\frac{\tan^2(\psi/4)}{\gamma^2} \tag{48}$$

and

$$\Omega_{\pm}^2=\frac{1-\gamma^2+\gamma^2\cos^2(\psi/4)\pm\sqrt{(\gamma^2-1)^2+2(\gamma^2+\gamma^4)\cos^2(\psi/4)-3\gamma^4\cos^4(\psi/4)}}{2\gamma^2}. \tag{49}$$

Clearly both Ω_0^2 and Ω_-^2 correspond to unstable solutions and must be discarded. Hence the correct frequency is given by Ω_+^2.

As in the semi-infinite case, the frequency corresponding to the Meissner state is obtained from that for the mixed state by setting $\gamma=1$. This results in the expression

$$\Omega^2=\frac{1}{2}\left[\cos^2\left(\frac{\psi}{4}\right)+\sqrt{4\cos^2\left(\frac{\psi}{4}\right)-3\cos^4\left(\frac{\psi}{4}\right)}\right], \tag{50}$$

which is independent of the magnetic field and depends only on the magnitude of the discontinuity of the phase ψ at the position of the inhomogeneity, i.e., on the strength of the impurity potential (see the discussion of Sec. V). Examining this expression, it can be seen that as the coupling strength ψ varies between 0 and 2π, the frequency decreases from its maximum (corresponding to the Josephson plasma frequency) to zero.

It can be shown quite generally that, irrespective of the coupling strength and the magnitude of the magnetic field, $\Omega^2_{\text{infinite}}-1\leqslant\Omega^2_{\text{inhomog}}\leqslant\Omega^2_{\text{infinite}}$, indicating that, as one would expect, the frequencies of the localized states always lie within the gap of the spectrum of the infinite system.[16] Parametric plots of the Ω^2 versus the magnetic field for the mixed and Meissner states for this situation are shown in Fig. 8 for two particular values of ψ.

Also in this case the behavior of the characteristic decay length λ can be determined. The result is plotted in Figs. 9 and 10 for the same values of ψ as in Fig. 8.

V. DISCUSSION AND CONCLUSIONS

We have shown that in the presence of phase impurities Tamm-like collective modes of the Josephson phase can exist in long Josephson tunneling junctions. These modes correspond to an oscillation of the Josephson vortex structure that becomes localized in the junction in the immediate proximity of the impurity. In the Meissner state this structure is described by Eq. (37), while, in the mixed state, the appropriate expression is given by Eq. (39).

The corresponding dispersion relations are shown in Fig. 8. These curves must be compared with the dispersion relations for infinite and semi-infinite junctions of Figs. 2 and 4. The modes of the infinite junction form a characteristic con-

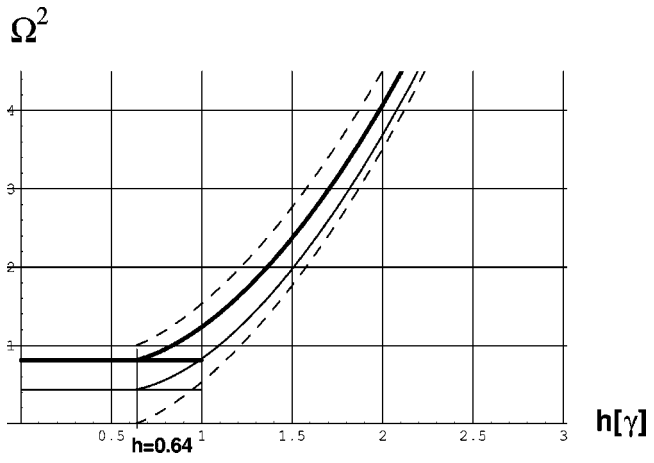

FIG. 8. The reduced frequency Ω^2 as a function of the magnetic field for the phase inhomogeneous junction in the mixed and Meissner states. For purposes of illustration, we have presented the plots for the values π (heavy line) and $3\pi/2$ for the phase discontinuity ψ. The dashed curves delimit the gap in the spectrum of the infinite system. The notation is the same as in Fig. 2.

tinuum in which a gap equal in magnitude to the Josephson plasma frequency is present (in terms of the reduced frequency, this gap is equal to unity). In Fig. 8 the location of the edges of such a continuum for the mixed state is marked by dashed lines: it is readily found that the upper edge is in our notation given by γ^{-2}, while the lower one is given by $\gamma^{-2}-1$. In the Meissner state a gap is present up to the plasma frequency threshold from where the continuum extends then to infinity. We have found that, as in the case of a semi-infinite junction, the frequency of the localized modes never enters this continuum so that the modes are well defined for all values of the external magnetic field.

Our results imply the following physical scenario as a function of the magnitude of the externally applied magnetic field. A semi-infinite junction is in the Meissner state for low fields whereupon a ''partial'' Josephson vortex exists at the surface, its integrated flux being less than one flux quantum

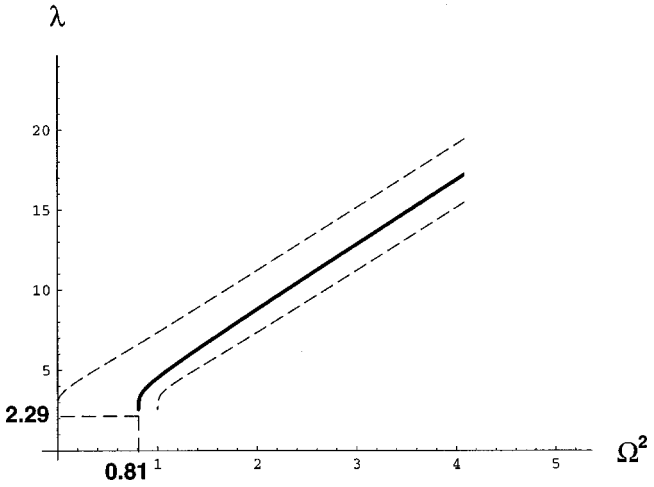

FIG. 9. Localized modes decay length vs the reduced frequency Ω^2 for the inhomogeneous system in the mixed state for a phase discontinuity of π. The curve is always seen to lie within the dashed lines which delimit the gap in the infinite spectrum. The notation is the same as in Fig. 2.

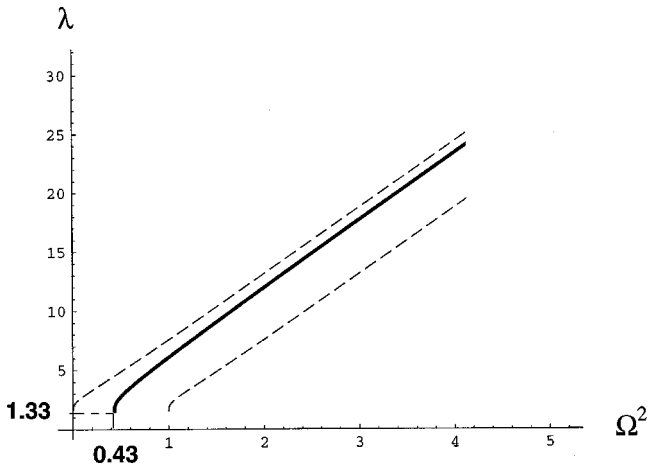

FIG. 10. Localized modes decay length vs the reduced frequency Ω^2 for the inhomogeneous system in the mixed state for a phase discontinuity of $3\pi/2$. The curve is always seen to lie within those delimiting the gap in the infinite spectrum. The notation is the same as in Fig. 2.

for all $0 \leqslant H \leqslant H_s$ (it is exactly a half quantum at the superheating field). As the field is increased, the restoring force keeping the ''partial-vortex'' localized at the surface reduces, causing a softening of the corresponding small oscillations frequency. When H reaches the lower critical field H_{c1} ($h=0.64$ in Fig. 4), vortex penetration occurs and the system in general enters the mixed state. However, as shown in Ref. 4, there exists a ''superheating field'' and the possibility of realizing a metastable Meissner state for fields in the range $H_{c1} \leqslant H \leqslant H_s$. For fields greater than H_{c1}, the frequency corresponding to the Meissner state continues to decrease until it finally vanishes at the superheating field. At this point a vortex can nucleate at the surface and, in the absence of a constraining force, is able to enter the bulk of the junction. This leads eventually to the formation of the mixed state.[25]

The results for a phase-inhomogeneous long Josephson junction show similar behavior in that the localized modes persist for all magnetic fields and for all strengths of coupling to the vicinal Abrikosov vortex (i.e., for all magnitudes of the phase discontinuity ψ). Also in this instance the trapped flux is less than a flux quantum and is proportional to ψ.[24] Unlike in the semi-infinite case, the frequency corresponding to the Meissner state in this instance is independent of the magnetic field. This is because, for a long junction with a phase-inhomogeneity far removed from the edges, there is no sensitivity in the Meissner regime to the applied field. Furthermore, in the Meissner state the frequency of the localized mode always lies below the Josephson plasma threshold.

The Tamm-like modes discussed in this article are characterized by a localization (or decay) length λ. In the case of a semi-infinite junction, this quantity is divergent at small applied fields (see Fig. 6 appropriate to the Meissner state) indicating that the mode extends throughout the system. λ decreases rapidly as the field is increased and is of the order of the Josephson penetration depth at the lower critical field H_{c1}. Continuing into the superheating regime, the decay length decreases to exactly λ_J at the superheating field H_s. At the lower critical field, the decay lengths in the mixed and

Meissner states coincide and are given by $\lambda \simeq 2.79\lambda_J$. The transition to the mixed regime is accompanied by a reversal in the trend as λ now begins to increase and diverges for large magnetic fields. This behavior is depicted in Fig. 5 for the semi-infinite junction, and in Figs. 9 and 10 for the phase inhomogeneous junction. In the latter case, the decay lengths are plotted against the reduced frequency for two representative values of the phase discontinuity.

A natural way to attempt a detection of the type of collective modes discussed in the present paper is represented by the study of the *I-V* characteristic where the small oscillation spectrum could be expected to manifest itself in the form of resonances. Work in this area has been intense.[26–31] To date, however, although much is known about large amplitude oscillations (mostly associated with solitonlike vortex motion),[32–34] unequivocal experimental evidence for the small oscillations modes is lacking.[35] It is also interesting to mention in the context of phase-inhomogeneous Josephson junctions that the presence of inhomogeneities and the associated current profile in Josephson junctions has been experimentally studied by Scheuermann and coworkers[36] using a laser scanning technique.

The problem explicitly treated in the present paper concerns isolated phase impurities. The effect of a finite density of phase impurities[15] on the small amplitude spectrum of a Josephson junction is also of considerable interest and has been addressed elsewhere.[37]

We conclude by noting that in the presence of phase impurities the standard description of the lower critical field is no longer applicable, as the closest impurity to the junction edges will lead to an effective junction length. Accordingly the phase diagram discussed in Ref. 4 must be revised in view of the fact that even in the limit of an infinitely long junction, the superheating field will not simply become the Ferrel-Prange critical field $\phi_0/2\pi\lambda_L\lambda_J$.[38]

[1] I. O. Kulik, Zh. Éksp. Teor. Fiz. **51**, 1952 (1966) [Sov. Phys. JETP **24**, 1307 (1967)].

[2] P. Lebwohl and M. J. Stephen, Phys. Rev. **163**, 376 (1967).

[3] A. L. Fetter and M. J. Stephen, Phys. Rev. **168**, 475 (1968).

[4] A. E. Gorbonosov and I. O. Kulik, Zh. Éksp. Teor. Fiz. **60**, 688 (1971) [Sov. Phys. JETP **33**, 374 (1971)].

[5] S. L. Miller, K. R. Biagi, J. R. Clem, and D. K. Finnemore, Phys. Rev. B **31**, 2684 (1985).

[6] O. B. Hyun, D. K. Finnemore, L. A. Schwartzkopf, and J. R. Clem, Phys. Rev. Lett. **58**, 599 (1987).

[7] O. B. Hyun, J. R. Clem, and D. K. Finnemore, Phys. Rev. B **40**, 175 (1989).

[8] V. N. Gubankov, M. P. Lisitskii, I. L. Serpuchenko, F. N. Sklokin, and M.V. Fistul, Supercond. Sci. Technol. **5**, 168 (1992).

[9] V. N. Gubankov, M. P. Lisitskii, I. L. Serpuchenko, and M. V. Fistul, Physica B **194-196**, 1697 (1994).

[10] A. A. Golubov and M. Yu. Kupriyanov, Zh. Éksp. Teor. Fiz. **92**, 1512 (1987) [Sov. Phys. JETP **65**, 849 (1987)].

[11] M. V. Fistul, Zh. Éksp. Teor. Fiz. **96**, 369 (1989) [Sov. Phys. JETP **69**, 209 (1989)].

[12] L. G. Aslamazov and E. V. Gurovich, Zh. Éksp. Teor. Fiz. **40**, 22 (1984) [JETP Lett. **40**, 746 (1984)].

[13] A. A. Golubov and A. V. Ustinov, Phys. Lett. A **162**, 409 (1992).

[14] M. V. Fistul and G. F. Giuliani, Phys. Rev. B **58**, 9343 (1998).

[15] M. V. Fistul and G. F. Giuliani, Phys. Rev. B **58**, 9348 (1998).

[16] I. Tamm, Phys. Z. Sowjetunion **1**, 733 (1932).

[17] A. Barone and G. Paterno, *Physics and Applications of the Josephson Effect* (Wiley, New York, 1982).

[18] I. O. Kulik and I. K. Yanson, *The Josephson Effect in Superconductive Tunneling Structures* (Israel Program for Scientific Translations, Jerusalem, 1972).

[19] J. C. Swihart, J. Appl. Phys. **32**, 461 (1961).

[20] E. T. Whittaker and G. N. Watson, *A Course of Modern Analysis* (Cambridge University Press, Cambridge, England, 1962).

[21] In referring to the Jacobian elliptic functions in what follows, the modulus will be omitted for brevity unless it differs from γ. Furthermore, the notation for the Jacobian elliptic integrals and functions followed in this article is that of Ref. 20.

[22] I. S. Gradshteyn and I. M. Ryzhik, *Table of Integrals, Series and Products* (Academic Press, New York, 1994).

[23] Equation (21) in Ref. 4 appears to have what we assume to be a typographical error. η_1 in the third term on the right hand side should be to the power unity, not the second power. A second apparent typographical error in Ref. 4 occurs in the expression for $\Omega_{\pm}^2$.

[24] It is readily found that the total flux associated with this phase distortion is given by $(\psi/2\pi)\phi_0$.

[25] A similar surface vortex nucleation picture has been discussed for the case of Josephson junction arrays in D.-X. Chen, J. J. Moreno, and A. Hernando, Phys. Rev. B **56**, 2364 (1997).

[26] T. V. RajeevKumar, J. -X. Przybysz, and J. T. Chen, Solid State Commun. **25**, 767 (1978).

[27] K. Hamasaki, K. Yoshida, F. Irie, K. Enpuku, and M. Inoue, J. Appl. Phys. **19**, 191 (1980).

[28] K. Hamasaki, K. Enpuku, F. Irie, and K. Yoshida, J. Appl. Phys. **52**, 6816 (1981).

[29] K. Yoshida, K. Hamasaki, K. Enpuku, and F. Irie, Physica B **109**, 2052 (1981).

[30] M. Cirillo, G. Costabile, S. Pace, and B. Savo, IEEE Trans. Magn. **19**, 1014 (1983).

[31] M. Scheuermann, J. T. Chen, and J. -J. Chang, J. Appl. Phys. **54**, 3286 (1983).

[32] J. T. Chen, T. F. Finnegan, and D. N. Langenberg, Physica (Amsterdam) **55**, 413 (1971).

[33] T. A. Fulton and R. C. Dynes, Solid State Commun. **12**, 57 (1973).

[34] G. Costabile, R. D. Parmentier, and B. Savo, Appl. Phys. Lett. **32**, 587 (1978).

[35] K. K. Likharev, *Dynamics of Josephson Junctions and Circuits* (Gordon and Breach, Montreux, 1986).

[36] M. Scheuermann, J. R. Lhota, P. K. Kuo, and J. T. Chen, Phys. Rev. Lett. **50**, 74 (1983).

[37] M. V. Fistul and G. F. Giuliani (unpublished).

[38] R. A. Ferrell and R. E. Prange, Phys. Rev. Lett. **10**, 479 (1963).